Supplementary Information accompanies the paper on *Nature's* website (http://www.nature.com).

Acknowledgements

We thank E. Allen, H. Chatterjee, J. Hooker, J. Mead, C. Potter and T. Yamada for access to specimens, and R. Barton, E. Blum, M. Colbert, C. Dean, J. DePonte, B. Frohlich, K. Grecco, K. H. Höhne, N. Jeffery, B. Jonsdottir, W. Jungers, R. Ketcham, K. Kupczik, D. Lieberman, Z. Luo, J. Moore, M. Muller, J. Neiger, C. Pellow, D. Plummer, A. Pommert, C. Ross, G. B. Schneider and A. Walker for their help. This research was supported by grants for the UCL Graduate School to F.S. and from the NSF to J.G.M.T. and S.T.H.

Competing interests statement

The authors declare that they have no competing financial interests.

Correspondence and requests for materials should be addressed to F.S. (e-mail: f.spoor@ucl.ac.uk).

Allometric cascade as a unifying principle of body mass effects on metabolism

Charles-A. Darveau*, Raul K. Suarez†, Russel D. Andrews* & Peter W. Hochachka*

** Department of Zoology, University of British Columbia, Vancouver, BC, V6T 1Z4, Canada*

† Department of Ecology, Evolution, and Marine Biology, University of California, Santa Barbara, California 93106-9610, USA

The power function of basal metabolic rate scaling is expressed as aM^b, where a corresponds to a scaling constant (intercept), M is body mass, and b is the scaling exponent. The 3/4 power law (the best-fit b value for mammals) was developed from Kleiber's original analysis[1] and, since then, most workers have searched for a single cause to explain the observed allometry. Here we present a multiple-causes model of allometry, where the exponent b is the sum of the influences of multiple contributors to metabolism and control. The relative strength of each contributor, with its own characteristic exponent value, is determined by the control contribution. To illustrate its use, we apply this model to maximum versus basal metabolic rates to explain the differing scaling behaviour of these two biological states in mammals. The main difference in scaling is that, for the basal metabolic rate, the O_2 delivery steps contribute almost nothing to the global b scaling exponent, whereas for the maximum metabolic rate, the O_2 delivery steps significantly increase the global b value.

Until now, the classical approach to the basal metabolic rate (BMR) allometry problem has been to search for the single driving force or single rate-limiting step enforcing its scaling behaviour on overall metabolism. However, this concept in metabolic regulation studies was abandoned during the 1960s and was replaced by the concept of multiple control sites in metabolic pathways. By the 1980s and 1990s, rigorous mathematical models allowed control analysis to quantify the control contributions of different steps in metabolic pathways[2–5] or in whole-organism physiological processes[6]. A key point, that control is vested in both energy supply and energy demand pathways[3–5], is important because many biologists estimate metabolic rate from O_2 uptake rates per gram per minute or from heat output rates. These parameter estimates are valid because they in turn are stoichiometrically related to complex pathways of adenosine triphosphate (ATP) synthesis rates and ATP utilization rates (however, see the discussion below on the 'O_2 wasting effect' of proton leak). In organisms at steady state the fluxes through ATP synthesis and utilization pathways are equal and mass-specific metabolic rate is equivalent to μmols ATP cycled through ATP supply and ATP demand pathways per gram per minute. That is why it should not be surprising that modern metabolic studies identify regulatory roles in overall metabolic fluxes in both energy-supply and energy-demand pathways[2–6]. In the traditional power function

$$\mathrm{BMR} = a\,M^b \qquad (1)$$

(a, M and b defined above), examination of the effects of body mass on metabolism should ideally consider the value of exponent b in equation (1) and the control contribution (or control coefficient) for each and every major step in ATP supply and ATP demand pathways in the system under investigation.

To sort out the varied contributions to control of net metabolic flux, say net O_2 flux, experimenters determine the fractional change in organismal O_2 flux caused by a fractional change in flux capacity through any given step or process in the path of O_2 from lungs to mitochondria in working tissues. The fractional change in organismal flux divided by the fractional change in capacity represents the control coefficient at each step[2–6]. To illustrate, if the O_2 flux capacity of the lung is increased by 50% but only a 25% change in overall O_2 flux is achieved, the control coefficient for lung diffusion is 0.5, equal to the fractional change in overall O_2 flux divided by the fractional change in lung flux capacity. All the control coefficients in the pathway by definition add up to 1. In a system with a classical single rate-limiting step, say O_2 delivery[7,8], the control coefficient for that step would be essentially 1; that is, all control is vested in this process. The latter situation is never found in metabolic systems of any complexity[3–6]. Under resting conditions all steps in the mammalian O_2 delivery chain necessarily display huge excess capacities and thus could not possibly be 'rate limiting' in the classical sense, while as we shall discuss further below, under maximum O_2 flux conditions, control is shared rather evenly among several major links in the chain. Hence the usually explicit, sometimes implicit, assumption of traditional allometry studies[7,8], that there is a single rate-limiting step or process that accounts for the b value in equation (1), is flawed.

We present here a multiple-causes model of allometry, in which there are multiple contributors to control, each with their own characteristic b values, that with their control contributions determine the value of the b scaling coefficient for overall energy metabolism. We can express this relationship as:

$$\mathrm{MR} = a\sum c_i M^{b_i} \qquad (2)$$

where MR is the metabolic rate in any given state, M is body mass, a is the intercept, b_i the scaling exponent of the process i, and c_i the control coefficient of the process i. (In most cases, a will be taken simply as the intercept, which is traditional in the allometry field. As ATP-utilizing processes are linked in parallel, each may have a unique a_i value; in sum these equal the baseline ATP turnover. On the energy supply side, the processes are linked in series with only one intercept at steady state indicating the same rate of baseline ATP turnover. For some purposes it is useful to decompose a into $a_{i,\max}$ the flux capacity through step i, and f_i the fraction of $a_{i,\max}$ used in a given metabolic state (see discussion below)).

Depending on metabolic state, the overall MR corresponds to the sum of the various contributors to ATP turnover, and the b exponent is the sum of the scaling exponents of all contributors, modulated by their control coefficients. In other words, each step in the linked series (that makes up the process, say O_2 flux, under study) possesses its own scaling behaviour, and its control coefficient c_i determines the degree to which its unique b_i exponent influences the global b value. For energy metabolism in mammals operating at varying rates between basal and maximum levels,

equation (2) applies to the sums of processes (such as ventilation, cardiac work, circulation) occurring at different sites in the body. At maximal sustainable work rates (equivalent to maximum sustainable ATP turnover rates), major contributors to control include the lung[6], the heart and circulation[9], cellular-level energy-supply pathways[3–5], which themselves have steps with low and high control contributions, and finally the ATP-demand pathways[3–5].

The concept of an allometric cascade arises from the layering of function at various levels of organization. The numerous steps involved in intracellular pathways of ATP demand and supply, each with its own characteristic b_i and c_i values, are at the base of the cascade. Other key steps, such as transporters, exchangers and pumps, function at the membrane-based cell surface, interfacing and integrating intra- and extracellular functions. Not all cells are identical of course, so another layering of function is found at organ and tissue levels of organization, where organ physiologies are integrated into organism BMR. Thus the overall scaling of BMR is a consequence of the interaction of scaling of these various 'functional units' involved in specific metabolic states. In short, we view this multi-cause model of scaling as an allometric cascade, with the b value for overall energy metabolism being determined by the c_i and b_i values for all major steps in the biochemical and physiological pathways of energy demand and energy supply that together make up whole-body MR. Application of this model to evaluate the scaling behaviour of MMR versus BMR illustrates its usefulness.

Our understanding of the control contribution of various steps in ATP demand and supply pathways under MMR conditions (often estimated as maximum oxygen consumption, $\dot{V}O_2$max) is better than our understanding of control of BMR. This is because the conditions of MMR—by definition, attained when further increments in work intensity do not correspond to further increments in $\dot{V}O_2$—are readily achievable and reproducible in numerous species. Recent careful statistical and physiological analyses[10] for a group of 'standardized' mammals ($\dot{V}O_2$max data standardized to a haemoglobin concentration equal to 15 g per 100 ml and heart mass equal to 1% of body mass) found a scaling coefficient equal to 0.879 ($\pm$0.02, 95% confidence limits); this b value is highly significantly different from the b value of 0.729 ($\pm$ 0.038) found for the BMR of the same group of species. This difference[11] between BMR and MMR scaling cannot be explained by single-cause scaling theories. To see if our allometric model can account for this difference, we need to analyse the b_i and c_i values for key controlling steps in energy turnover in both conditions. The linked steps on the ATP supply side[3,4,6] are ventilation, pulmonary diffusion, cardiac output and circulation and capillary-tissue diffusion, plus fuel transfer to cellular catabolic processes in muscles (including fuel mobilization and O_2 transfer to, and consumption by, mitochondria). The b_i coefficients for most of these steps are known and range from ~0.7 to ~1.0, and the best available evidence indicates that at MMR control is distributed throughout the energy delivery chain (c_i values ranging from ~0.1 to ~0.3 (see Methods)).

For energy demand, the situation under MMR conditions is somewhat simplified since over 90% of O_2 consumption[2,11] is directed towards ATP synthesis for muscle work; that is, for actomyosin ATPase and the Ca^{2+} pump. Scaling studies have usually focused mainly on energy-supply processes, which at MMR may display moderate to zero reserve capacity. In fact, the functional capacities of O_2 delivery systems can sometimes be surpassed. For example, during intense exercise in some human athletes, the functional capacity of the lung at $\dot{V}O_2$max is breached and a condition termed 'desaturation' is observed, (blood passing through the lung cannot become fully saturated[2]); yet, because the short-fall can be made up by adjusting cardiac output and O_2 extraction, $\dot{V}O_2$ can still increase beyond this point. A similar situation can develop for the heart and circulation, which is also resolved by adjusting the sharing of control. (The maximum metabolic rates per gram of a small muscle mass can increase 2–3-fold above mass-specific rates under whole-body MMR conditions because a larger fraction of cardiac output can be directed to a smaller O_2-demand site[2]. This means that at whole-body MMR, capillary-mitochondria diffusion and mitochondrial metabolism per se retain reserve capacity.) Despite these adjustments, there is no doubt that at maximum aerobic exercise, O_2 delivery by the lung and heart must be close to an 'upper ceiling'. In contrast, under MMR conditions, actomyosin and Ca^{2+} pump must still display a huge reserve capacity; this is because of the requirement for over 3-fold higher[2] anaerobic than aerobic ATP turnover rates, primed by the glycolytic path or by phosphocreatine mobilization. Because of these contrasting conditions in the energy-supply versus energy-demand processes as aerobic maximum fluxes are approached, it is not surprising that the control contributions for energy supply increase (as in sum they approach classical rate-limiting function), while those for energy-demand processes under aerobic MMR conditions diminish towards zero[2,4]. That is why in Fig. 1, to see how they affect scaling we use two c_i values, 0.63 versus 0 and 0.28 versus 0, for actomyosin and Ca^{2+} cycling, respectively.

When the b_i and c_i values for all the above processes are used in equation (2) to see how they contribute to global b values for MMR, we calculate b values that range between 0.92 (b_{max}) to 0.82 (b_{min}), as the c_i values for actomyosin and Ca^{2+} ATPases shift from zero to maximum estimates (Fig. 1). Global b values in the ~0.8 to ~0.9 range are similar to empirically observed b scaling coefficients[11] as well as for MMR data that are standardized with respect to haemoglobin concentration and heart size[10]. Thus our model accommodates $\dot{V}O_2$max data that show high scaling coefficients for MMR compared to BMR. However, this remains a difficulty in allometric models[7,8] that assume that constraint on a single function—oxygen delivery—enforces the major b value on metabolism and on all other physiological rate processes. Instead of a physiological delivery system serving as a single rate-limiting process, as required by such models[7,8], *in vivo* the empirically observable operational rule of thumb seems to involve sharing of control, with regulatory contributions arising at many key steps in carbon flux, in O_2 flux and in ATP turnover[3,6].

Application of the multi-site model to BMR scaling is more difficult because less is known about the control of BMR than of MMR. To identify a starting point, we need to review what processes add up to the whole-body metabolism we refer to as BMR. In the laboratory rat, ~70% of basal whole-body O_2 consumption is used by the mitochondria to produce ATP for several ATP sinks, including protein turnover, Na^+ pump, Ca^{2+} pump, myosin ATPases, gluconeogenesis, ureagenesis, messenger RNA synthesis, and substrate cycling, contributing approximately 20–25, 20–25, 5, 5, 7, 2.5, <2, and <2%, respectively[12], to BMR.

For energy supply under BMR conditions all the oxygen-delivery steps display a huge excess capacity; this reserve capacity is what allows a 10-fold or more metabolic scope for activity in most animals and is a major reason why (as physiologists have long realised) these steps have minimal effects on the control of metabolism under BMR conditions[2,10]. Thus, for simulation purposes the c_i values for all the oxygen-delivery steps could be assumed to be zero. If any step were omitted, metabolic fluxes would fall to zero, so it is clear that some control contribution must arise from each of the oxygen-delivery steps, despite their huge excess capacity for oxygen delivery. That is why, in Fig. 1, small but finite c_i values are selected for each of the O_2 delivery steps; if these were set at zero, our overall conclusions, however, would not change.

It should be obvious, given such low c_i estimates for energy supply, that the b_i and c_i values for these steps will contribute little to the global b exponent for BMR (Fig. 1). To find the proximate determinants of the global b value for BMR we must examine the energy demand processes.

For energy demand in the ATP turnover cycle, under BMR

conditions the two major energy sinks, as already mentioned, are the Na^+ K^+ ATPase and protein turnover[12,13], for which b_i values of 0.72 and 0.77, respectively, are available in the literature (see Methods). For Na^+ K^+ ATPase, c_i values for various tissues vary, so, as explained in the Methods, we use two values, 0.70 and 0.35, to see the effect on the global b value. For protein synthesis the two corresponding c_i values are 0.10 and 0.30, values that bracket the percentage contribution to overall BMR. Finally, for completion we estimate c_i values for the Ca^{2+} pump, for ureagenesis, and for gluconeogenesis; these too are selected to be similar to their percentage contribution to overall BMR.

Using such estimated b_i and c_i values for energy supply and energy demand processes in equation (2), the global b for BMR equals 0.76 when the Na^+ K^+ ATPase control coefficient is 0.70, and this global b value increases to 0.79 when a control coefficient of 0.35 is associated with this step (Fig. 1b). Our estimates for Na^+ K^+ ATPase c_i values are conservative and values closer to unity may be appropriate[13], in which case the global b values for BMR would be even lower. These ranges of global b coefficients are in accord with the well-known 3/4 power law, but are generated largely by b_i and c_i values for ATP-demand processes. They are not generated by constraints imposed by O_2 supply systems, or any other single factor, in contrast to assumptions of most single-cause allometry models. As far as we know, aside from our multiple-causes model, no other allometric models have been able to explain these differing BMR versus MMR scaling patterns. One earlier series of studies[11] did emphasize the importance to allometry of co-adaptation of multiple steps in the path of O_2 from air to mitochondria. When viewed from a scaling perspective, we consider that the Weibel–Taylor model (of the matching of several functional links in O_2 flux control[11]) forms a kind of conceptual base for our currently proposed multi-site model of allometry.

Like Na^+ K^+ ATPase, the specific activities of many components in the complex pathways of energy supply and energy demand display b_i scaling coefficients close to 0.75, but many do not. For example, in mammals, citrate synthase scales with the value of b_i equal to about 0.9; several other enzymes show their own unique scaling b_i coefficients, and of course their own c_i control coefficients[2]. When coupled or integrated together into a unitary functional system, one could well expect that the b_i and c_i values for the dominant control sites could add up to global b values for metabolism that varied significantly from 0.75. The recent exhaustive analyses of BMR in 487 mammal species, arranged in zoogeographical clusters, show that this variation in b values for whole-body BMR is indeed observed[14]. Many of the factors contributing to this variation are referred to in our model as 'intrinsic' or 'extrinsic' to the proximate metabolic processes accounting for specific allometric behaviours.

Intrinsic factors influencing scaling can be found at various levels of the functional units. For example, not only is the organ-mass scaling pattern organ-specific, but the respiration rate of tissue slices of various organs also follow different, tissue-specific scaling expo-

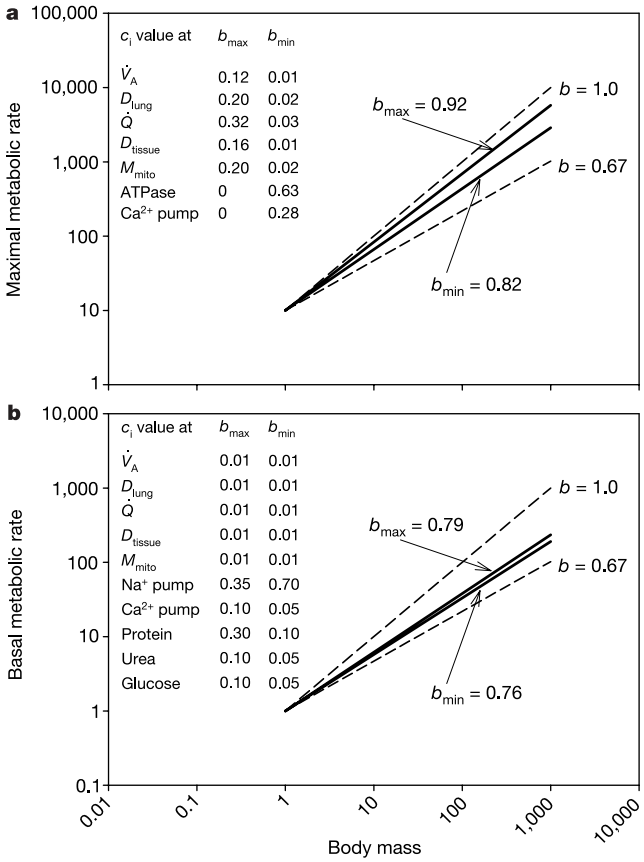

Figure 1 Estimates of b values for maximum and basal metabolic rates in mammals using the multi-site allometry model. The scaling patterns of the maximum and basal metabolic rates (MMR and BMR) were calculated from simulations solving equation (2) using c_i values shown in **a** and **b** (see Methods for b_i values). **a**, For MMR the functions listed in order are alveolar ventilation ($\dot{V}_A$), pulmonary diffusion (D_{lung}), cardiac output ($\dot{Q}$), capillary-mitochondria tissue diffusion (D_{tissue}), cytosolic and mitochondrial metabolism (M_{mito}) plus actomyosin ATPase (ATPase) and the Ca^{2+} pump. The same abbreviations are used in **b**, in addition to the Na^+ pump and protein, urea and glucose synthesis. The two sets of c_i values yield estimates of maximum (b_{max}) and minimum (b_{min}) values for scaling of MMR and BMR. For simulation purposes, metabolic rates and body mass are given in arbitrary units and the intercept for MMR (a) is assumed to be 10-fold higher than for BMR[10,11] (arbitrarily set at 1). For reference, slopes of 1.0 and 0.67 are shown in **a** and **b**.

nents[13]. These studies confirm differential scaling of various organs and their mitochondrial membrane content, both of which undoubtedly contribute to the scaling of the metabolic rate.

Variation in membrane composition is another intrinsic factor that may influence scaling coefficients. In mammals at rest, 10% of the oxygen consumed by the animal is non-mitochondrial, while another 20% of the O_2 consumed is used to maintain mitochondrial membrane potential affected by the leak of protons[12]. Allometric scaling of proton leak across the mitochondrial inner-membrane displays a b_i exponent of 0.86 in mammals[15]. This b_i estimate may not be statistically different from 0.75. However, at least tentatively, we assume that the trend is valid, since proton leakiness can be influenced by membrane composition[16], and percentage saturation of biological membranes increases[13] as body size increases. Although more work is required, it is already evident that membrane composition provides another example of intrinsic effects on metabolic rate, and on scaling not only of the proton leak, but also of the scaling of transport proteins such as Na^+ K^+ ATPase[13].

Although the same, coupled steps usually contribute to the metabolic characteristics of tissues and organs, their quantitative contributions to control may vary in different states. For example, insulin (and presumably endocrines generally) and the kinds of fuels used are intrinsic factors that influence flux rates through specific pathways (such as glycolysis or fatty acid oxidation) and modify control contributions of different sites in ATP turnover[2].

We mentioned above that the intercept may be viewed as being formed from two ($a_{i,\max}$ and f_i) parameters. This subdivision is important when looking across taxa, where current data show that both $a_{i,\max}$ and f_i parameters also can be modified. As an example, Suarez *et al.*[17] observed that when comparing among groups (from relatively sluggish fish to super-active bees), each with varying glycolytic flux rates, not only the maximal catalytic capacity of several enzyme sites in glycolysis increased, but at MMR there was also an increase in f_i or fractional velocity. Similarly, when comparing distant groups like ectotherms and endotherms, similar b exponents are observed but an obvious difference in intercept is found. This difference in baseline is in part due to differences in the cost associated with Na^+ ion pumping for which $a_{i,\max}$ is higher in endotherms but f_i is conserved[13].

Field biologists frequently emphasize that factors such as temperature, pressure, nutritional preferences, water availability and other ecological factors may be 'ultimate causes' or 'ultimate explanations' for why specific groups of organisms show specific allometric behaviour. Appeal, for example, is made to this level of explanation for different scaling exponents for field metabolic rates when comparing reptiles, birds and mammals[18]. Such 'ultimate' explanations also apply to the phylogenetically or environmentally linked scaling patterns noted by Lovegrove[14]. We interpret all such forces (in addition to purely abiotic ones such as temperature, hydrostatic pressure or osmotic pressure) as extrinsic factors that affect scaling relations by acting on a, b_i, and/or c_i in equation (2) above. So-called 'ultimate causes' thus are not 'causes' in a mechanistic sense, but only in the sense that they act through 'proximal causes' or 'proximal mechanisms' such as those outlined in our model.

In summary, then, most earlier analyses of scaling of metabolic and physiological processes have looked for a single process which scales with a universal b exponent; their models then assumed that this single process enforces the scaling behaviour for all other biochemical and physiological rate functions. We here refer to all such interpretations as single-cause models of scaling. The only way these could be valid is if the selected single process behaved as a master rate-determining step in metabolism and physiology, a concept that has long been abandoned in metabolic regulation research. Taken literally, if a single process, such as O_2 or fuel delivery, is rate-limiting for BMR, there can be no room left for scope for activity: higher metabolic rates would be blocked by this one process because it would already be rate-limiting even at rest. For this reason and many others[2], the concept of a master rate-limiting step was replaced by concepts of multi-site controls, with many processes contributing in varying degree to regulation of overall whole-organism metabolic and physiological rates[2–6]. When applied to the problem of scaling, the multi-site concept of allometry states that two key parameters (b_i, the scaling exponent and c_i, the control coefficient in equation (2)) for all major control sites in ATP-turnover pathways determine the overall scaling behaviour of whole-organism bioenergetics. For mammals, including humans, these values can be estimated for many of the key steps in energy turnover under two states, BMR and MMR. Our model supplies a mechanistic basis for why the scaling patterns of BMR and MMR differ: in scaling of BMR, the O_2 delivery steps contribute almost nothing to the global b scaling exponent, which is therefore largely determined by energy-demand processes, whereas at MMR, the O_2 delivery steps, now coupled to different ATPases, significantly increase the global b scaling coefficient. □

Methods

Estimating b_i and c_i values for MMR

For energy supply, the b_i and c_i values are estimated from data[9] for human $\dot{V}O_2max$ performance. In these analyses, control contributions from cell metabolism were ignored. However, we assume that mitochondrial metabolism displays a c_i value well above zero (for example, training increases mitochondrial volume by ~25% which correlates with a ~5% increase in $\dot{V}O_2max$[2,3], indicating a c_i value of ~0.2). To accommodate the mitochondrial data and to have all the c_i estimates add up to 1.0 in exercising humans, the estimates from ref. 9 must be multiplied by 1/1.2 or 0.8. Thus for alveolar ventilation $b_i = 0.80$ (ref. 19) and $c_i = 0.12$ (ref. 6; or 0.16 from ref. 9 × 0.8). For pulmonary diffusion, $b_i = 1.08$ (ref. 11) and $c_i = 0.20$ (ref. 9). For cardiac output[20], $b_i = 0.879$ while $c_i = \sim 0.32$ (ref. 9). Capillary volume densities scale with $b_i = 0.89$ (ref. 11), with $c_i = 0.20$ (ref. 9) for O_2 diffusion from capillaries to mitochondria. Mitochondrial volume densities and hence their maximum oxygen consumption rates scale with $b_i = 0.87$ (ref. 11), whereas $c_i = \sim 0.16$ (refs 2, 3).

For energy demand, under MMR conditions over 90% of O_2 consumption[2,11] is directed towards ATP synthesis for muscle work; that is, for actomyosin ATPase and the Ca^{2+} pump. What we need to complete our calculations are b_i and c_i values for both of these major ATP sinks. For actomyosin ATPase, $b_i = 0.77$ (ref. 21), and at low-to-moderate exercise intensities it contributes significantly to the control of overall metabolic rates[3–5]. Allometric data on the Ca^{2+} pump are also not abundant, but because muscle contraction frequency is directly correlated with this activity, an *in vivo* estimate of $b_i = 0.86$ ($r = 0.99$) is provided by scaling of stride frequency in a mouse-to-horse range of body sizes[22]. Similar scaling coefficients are obtained for the Ca^{2+} pump catalytic capacities in hearts of small and large animals[23]. Estimates of c_i values for actomyosin and Ca^{2+} ATPase can be obtained by comparing the impact of change in their capacities upon tissue respiration. Actomyosin concentrations and activities are 3–4-fold higher in FOG (fast twitch oxidative glycolytic) fibres than in slow fibres[3], while Ca^{2+} pump densities are about 1.7-fold higher[24]; together these can 'drive' O_2 delivery about 2.4 times faster[25,26] (linear over a broad range of submaximal work rates). Actomyosin accounts for a 1.92-fold increase in activation, and Ca^{2+} cycling accounts for the rest (~48% of the activation). Thus under these conditions, the c_i value (change in overall metabolic flux achievable/change in actomyosin catalytic capacity) equals 1.92/3.0 or 0.63, while for the Ca^{2+} pump the c_i equals ~0.48/1.7 or ~0.28. These values are calculated with respect to O_2 flux, so in total the two processes contribute up to 91% of the control under submaximal work. However, because c_i values may approach zero at MMR[4], in our simulations, we used two c_i values for actomyosin and Ca^{2+} ATPases, 0.63 versus 0 and 0.28 versus 0, respectively. A summary of these values is given in Fig. 1a.

Estimating b_i and c_i values for BMR

For energy supply under BMR conditions all the oxygen-delivery steps display a huge excess capacity[10]. Thus, small but finite c_i values were selected for each of these steps. The b_i and c_i values chosen for alveolar ventilation[19] are $b_i = 0.80$ and $c_i = 0.01$. For pulmonary diffusion[6,11], $b_i = 1.08$ and $c_i = 0.01$. For cardiac output[20] $b_i = 0.76$ and $c_i = 0.01$. For diffusion from capillaries to mitochondria, $b_i = 0.89$ (as above), whereas $c_i = 0.01$. For mitochondrial O_2 consumption, we were confronted with the issue of what state the mitochondria operate in under BMR conditions. As indicated above, state-3 mitochondrial respiration (saturated with all required substrates) is expected to scale to the 0.87 power. However, a positive scaling has been found[16] for the respiratory control ratio (RCR), with a b_i value of 0.121, indicating that state-4 respiration (which may be a probable state for many mitochondria under BMR conditions) scales with a lower exponent than state 3. Thus we considered that b_i values of $0.87 - 0.12 = 0.75$ and c_i values of about 0.01 would be reasonable estimates for mitochondrial respiration under BMR conditions.

For the energy demand of the ATP turnover cycle, under BMR conditions the two major energy sinks are the Na^+ K^+ ATPase and protein turnover[12,13]. For Na^+ K^+ ATPase, studies[13] determined an *in vivo* $b_i = 0.72$ and, in our simulation, the c_i was chosen to vary from 0.70 to 0.35. Estimates of c_i values for Na^+ K^+ ATPase can be obtained by comparing

the impact of change in $Na^+ K^+$ ATPase capacity upon tissue respiration. In vertebrate liver, a 5.6-fold change in $Na^+ K^+$ ATPase capacity 'drives' a 1.63-fold change in $\dot{V}O_2$, while in vertebrate brain, a 3.78-fold change in $Na^+ K^+$ ATPase 'drives' a 1.63-fold change in $\dot{V}O_2$; thus the ratios of change in metabolic flux capacities/change in $Na^+ K^+$ ATPase capacities, the c_i values, are 0.29 (for liver) and 0.43 (for brain). We do not have global c_i values for whole-body rates, but because $Na^+ K^+$ ATPase activities account for a large percentage of BMR in numerous animals[12,13], the c_i values estimated for the liver and brain are probably fairly representative. In some tissues, such as kidneys, the values may be higher; in some, such as non-working muscles, they may be lower[13]. That is why, in our simulation (Fig. 1), two widely differing c_i values, 0.70 and 0.35, are used to illustrate the effect on overall scaling behaviour.

A second major energy-demand process under BMR conditions is protein synthesis. Previous allometric studies of protein synthesis rates establish $b_i = 0.77$ (refs 27, 28), but experimental studies allowing quantifying c_i coefficients for this process are not abundant. Nevertheless, *in vitro* studies[29] provide a c_i value of 0.11 for protein synthesis in liver slices of amphibians. In humans and rats, whole-organism studies of protein synthesis and metabolism usually find c_i values that are somewhat higher[2]. For our simulation, with the $Na^+ K^+$ ATPase c_i set at 0.70, we selected for protein synthesis a value of $c_i = 0.10$. To complete our simulation, we also included data for three more ATP demand processes: Ca^{2+} ATPase plus urea and glucose biosyntheses. As above, a value of $b_i = 0.86$ ($r = 0.99$) (ref. 22) is our best current estimate for the Ca^{2+} pump, while because of a low contribution to BMR we assume a relatively low value of $c_i = 0.05$. For urea synthesis[28] $b_i = 0.77$ and we selected $c_i = 0.05$. Similarly, for gluconeogenesis[30], $b_i = 0.76$ and we selected $c_i = 0.05$; the latter two c_i values are again similar to the percentage contributions of these processes to BMR[12]. We consider these low estimates to be reasonable, because so far, no studies have found large contributions of ureagenesis or glucogenesis to the control of basal metabolism[3–5,12]. With the $Na^+ K^+$ ATPase c_i value set at 0.7, the values for all the ATP demand processes are then 0.10, 0.05, 0.05 and 0.05 respectively; these double when the $Na^+ K^+$ ATPase c_i value is reduced to 0.30 (Fig. 1b). The two c_i values for protein synthesis bracket the percentage contribution[12] of this ATP demand process to BMR. A summary of these values is given in Fig. 1b.

Received 5 September 2001; accepted 20 February 2002.

1. Kleiber, M. Body size and metabolism. *Hilgarida* **6,** 315–353 (1932).
2. Hochachka, P. W. & Somero, G. N. *Biochemical Adaptation—Mechanism and Process in Physiological Evolution* (Oxford Univ. Press, New York, 2002).
3. Hochachka, P. W. *Muscles as Molecular and Metabolic Machines* (CRC Press, Boca Raton, Florida, 1994).
4. Jeneson, J. A., Westerhoff, H. V. & Kushmerick, M. J. A metabolic control analysis of kinetic controls in ATP free energy metabolism in contracting skeletal muscle. *Am. J. Physiol. Cell Physiol.* **279,** C813–C832 (2000).
5. Thomas, S. & Fell, D. A. A control analysis exploration of the role of ATP utilisation in glycolytic-flux control and glycolytic-metabolite-concentration regulation. *Eur. J. Biochem.* **258,** 956–967 (1998).
6. Jones, J. H. Optimization of the mammalian respiratory system: symmorphosis versus single species adaptation. *Comp. Biochem. Physiol. B* **120,** 125–138 (1998).
7. West, G. B., Brown, J. H. & Enquist, B. J. The fourth dimension of life: fractal geometry and allometric scaling of organisms. *Science* **284,** 1677–1679 (1999).
8. Banavar, J. R., Maritan, A. & Rinaldo, A. Size and form in efficient transportation networks. *Nature* **399,** 130–132 (1999).
9. Wagner, P. D. Algebraic analysis of the determinants of $\dot{V}O_2$ max. *Resp. Physiol.* **93,** 221–237 (1993).
10. Bishop, C. M. The maximum oxygen consumption and aerobic scope of birds and mammals: getting to the heart of the matter. *Proc. R. Soc. Lond. B* **266,** 2275–2281 (1999).
11. Weibel, E. R. *Symmorphosis, on Form and Function Shaping Life* (Harvard Univ. Press, Cambridge, 2000).
12. Rolfe, D. F. S. & Brown, G. C. Cellular energy utilization and molecular origin of standard metabolic rate in mammals. *Physiol. Rev.* **77,** 731–758 (1997).
13. Hulbert, A. J. & Else, P. L. Mechanisms underlying the cost of living in animals. *Annu. Rev. Physiol.* **62,** 207–235 (2000).
14. Lovegrove, B. G. The zoogeography of mammalian basal metabolic rate. *Am. Nat.* **156,** 201–219 (2000).
15. Porter, R. K. & Brand, M. D. Body mass dependence of H^+ leak in mitochondria and its relevance to metabolic rate. *Nature* **362,** 628–630 (1993).
16. Porter, R. K., Hulbert, A. J. & Brand, M. D. Allometry of mitochondrial proton leak: influence of membrane surface area and fatty acid composition. *Am. J. Physiol.* **271,** R1550–R1560 (1996).
17. Suarez, R. K., Staples, J. F., Lighton, J. R. B. & West, T. G. Relationship between enzymatic flux capacities and metabolic flux rates: Non-equilibrium reactions in muscle glycolysis. *Proc. Natl Acad. Sci. USA* **94,** 7065–7069 (1997).
18. Nagy, K. A., Girard, I. A. & Brown, T. K. Energetics of free-ranging mammals, reptiles, and birds. *Annu. Rev. Nutr.* **19,** 247–277 (1999).
19. Stahl, W. R. Scaling of respiratory variables in mammals. *J. Appl. Physiol.* **22,** 453–460 (1967).
20. Bishop, C. M. Heart mass and the maximum cardiac output of birds and mammals: implications for estimating the maximum aerobic power input of flying animals. *Phil. Trans. R. Soc. Lond. B* **352,** 447–456 (1997).
21. Lindstedt, S. L., Hoppeler, H., Bard, K. M. & Thornson, H. A. Jr Estimates of muscle-shortening rate during locomotion. *Am. J. Physiol.* **249,** R669–R703 (1985).
22. Heglund, N. C., Taylor, C. R. & McMahon, T. A. Scaling stride frequency and gait to animal size: mice to horses. *Science* **186,** 1112–1113 (1974).
23. Hamilton, N. & Ianuzzo, C. D. Contractile and calcium regulating capacities of myocardia of different sized mammals scale with resting heart rate. *Mol. Cell. Biochem.* **106,** 133–141 (1991).
24. Szentesi, P., Zaremba, R., van Mechelen, W. & Stienen, G. J. M. ATP utilisation for calcium uptake and force production in different types of human skeletal muscle fibres. *J. Physiol. Lond.* **531,** 393–403 (2001).
25. Armstrong, R. B. & Laughlin, M. H. Metabolic indicators of fibre recruitment in mammalian muscles during locomotion. *J. Exp. Biol.* **115,** 201–213 (1985).
26. Hochachka, P. W., Bianconcini, M., Parkhouse, W. D. & Dobson, G. P. On the role of actomyosin ATPase in regulation of ATP turnover rates during intense exercise. *Proc. Natl Acad. Sci. USA* **88,** 5764–5768 (1991).
27. Waterlow, J. C. Protein turnover with special reference to man. *Q. J. Exp. Physiol.* **69,** 409–438 (1984).
28. Brody, S. *Bioenergetics and Growth* (Hafner, New York, 1945).
29. Fuery, C. J., Withers, P. C. & Guppy, M. Protein synthesis in the liver of *Bufo marinus*—cost and contribution to oxygen consumption. *Comp. Biochem. Physiol. A* **119,** 459–467 (1998).
30. Weber, J. M., Fournier, R. & Grant, C. Glucose kinetics of the Virginia possum: Possible implications for predicting glucose turnover in mammals. *Comp. Biochem. Physiol.* **118,** 713–719 (1997).

Acknowledgements

P.W.H. and R.D.A. were supported by the NSERC, Canada; R.K.S. by the NSF in the USA. C.-A.D. was an NSERC and FCAR pre-doctoral fellow.

Competing interests statement

The authors declare that they have no competing financial interests.

Correspondence and requests for materials should be addressed to P.W.H. (e-mail: pwh@zoology.ubc.ca).

Host plants influence parasitism of forest caterpillars

J. T. Lill*, R. J. Marquis & R. E. Ricklefs

Department of Biology, University of Missouri–St. Louis, St. Louis, Missouri 63121, USA

Patterns of association between herbivores and host plants have been thought to reflect the quality of plants as food resources[1,2] as influenced by plant nutrient composition[3], defences[4,5], and phenology[6]. Host-plant-specific enemies, that is, the third trophic level, might also influence the distribution of herbivores across plant species[7–10]. However, studies of the evolution of herbivore host range[11–15] have generally not examined the third trophic level, leaving unclear the importance of this factor in the evolution of plant–insect herbivore interactions[16]. Analysis of parasitoid rearings by the Canadian Forest Insect Survey shows that parasitism of particular Lepidoptera species is strongly host-plant-dependent, that the pattern of host-plant dependence varies among species of caterpillars, and that some parasitoid species are themselves specialized with respect to tree species. Host-plant-dependent parasitism suggests the possibility of top-down influence on host plant use. Differences in parasitism among particular caterpillar–host plant combinations could select for specialization of host plant ranges within caterpillar communities. Such specialization would ultimately promote the species diversification of Lepidoptera in temperate forests with respect to escape from enemies.

Here, we test the hypothesis that a caterpillar's host plant influences the identity of its parasitoid enemies and its probability of being parasitized. Our analysis includes a broad range of forest tree species and their associated caterpillar and parasitoid species in southern Ontario and Quebec, Canada, taking advantage of the extensive data set generated by the Canadian Forest Insect Survey[17] (CFIS). Because parasitoids almost always kill their hosts, evidence of host-plant-specific parasitism indicates that members of the third trophic level can influence the suitability of host plants for herbivore

* Present address: Washington University, Tyson Research Center, PO Box 258, Eureka, Missouri 63025, USA.